CHEMMEDCHEM
Chemistry & Drug Discovery

Supporting Information

Structural Characterization and Computer-Aided Optimization of a Small-Molecule Inhibitor of the Arp2/3 Complex, a Key Regulator of the Actin Cytoskeleton

Andrew W. Baggett,[a] Zoe Cournia,[b] Min Suk Han,[a] George Patargias,[b] Adam C. Glass,[a] Shih-Yuan Liu,[a] and Brad J. Nolen*[a]

cmdc_201200104_sm_miscellaneous_information.pdf

Supplementary Table 1: X-ray crystallography data collection and refinement statistics

Data Collection	
Beamline	BL 5.0.1
Resolution (Å)	20.0-2.48
Space group	$P2_12_12_1$
Cell constants	a = 111.19
	b = 129.69
	c = 205.00
Mosaicity (˚)	0.45
Measured reflections	1027196
Ubique reflections	93,952
Mean I/σ	19.6/3.1
R_{sym} (%)[a]	6.3/37.8
Completeness (%)	88.7/74.7
Refinement	
Modeled residues	1923
Water molecules	221
Average B-factor (Å^2)	
main chain	44.4
side chain	45.4
inhibitor	42.6
water	35.0
RMS from ideal	
bond lengths	0.008
bond angles	1.4
Ramachandran plot	
most favored	1334
additionally allowed	163
generously allowed	11
disallowed	0
R_{free}	26.1
R_{work}[b]	22.1

[a] $R_{sym} = \Sigma|I_h - \langle I_h \rangle| / \Sigma I_h$, where $\langle I_h \rangle$ is the average intensity over symmetrically equivalent reflections.
[b] $R_{work} = \Sigma ||F_o|-|F_c|| / \Sigma F_o$, where F_o is an observed amplitude and F_c a calculated amplitude; R_{free} is the same statistic calculated over a subset (5%) of the data that have not been used for refinement.

Supplementary Table 2: Predicted Properties from *QikProp* for **1** and its analogs.

Compound	MW [a]	QP log *P* [b]	QP log *S* [c]	QP PCaco [d]
1	296.343	3.835	-4.646	1,564.440
2	312.343	3.166	-3.721	772.960
3	330.789	4.771	-6.036	2,095.861
4	326.370	4.062	-4.399	2,550.883
5	312.343	3.488	-4.879	654.939
6	330.789	4.431	-5.002	2,457.463
7	312.798	4.217	-4.602	2,331.180
8	330.789	4.289	-4.701	2,460.804
9	326.370	3.915	-4.087	2,471.665
10	312.798	4.165	-4.533	2,632.276
11	312.798	4.058	-4.221	2,346.557

[a] Molecular weight. [b] Predicted octanol/water log *P*. [c] Predicted aqueous solubility; *S* in mol/L. [d] Predicted Caco-2 cell permeability in nm/s.

Supplementary Table 3: Forward and reverse mutations for compounds **3, 6, 7, 8, 10, 11**. Hysteresis is found to be between 0.04 and 0.5 kcal/mol for all cases.

Compound	ΔG bound (kcal/mol)	ΔG unbound (kcal/mol)	ΔΔG total (kcal/mol)
3	-3.35 ± 0.12	0.25 ± 0.09	3.6 ± 0.28
3 – reverse	3.56 ± 0.15	0.26 ± 0.09	-3.8 ± 0.24
6	2.44 ± 0.09	2.56 ± 0.08	0.12 ± 0.12
6 – reverse	-2.12 ± 0.11	-2.4 ± 0.09	-0.28 ± 0.14
7	10.0 ± 0.13	8.54 ± 0.1	-1.46 ± 0.16
7 – reverse	9.84 ± 0.13	8.32 ± 0.1	1.52 ± 0.16
8	-0.87 ± 0.11	1.05 ± 0.08	1.92 ± 0.14
8 – reverse	0.84 ± 0.11	-1.17 ± 0.09	-2.01 ± 0.14
10	-5.0 ± 0.12	-1.1 ± 0.09	3.9 ± 0.15
10 – reverse	-4.58 ± 0.11	1.1 ± 0.09	-3.47 ± 0.14
11	7.4 ± 0.12	9.9 ± 0.11	2.5 ± 0.16
11 – reverse	-7.5 ± 0.13	-10.5 ± 0.11	3.0 ± 0.17

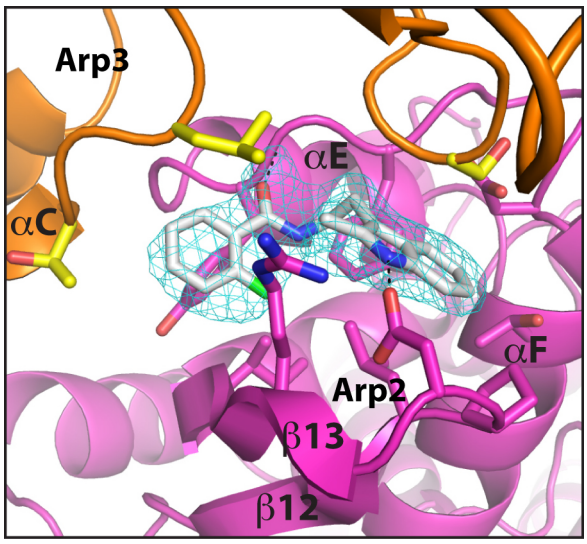

Supplementary Figure 1: CK-666 binding pocket showing an electron density map contoured at 2.0 σ for CK-666. The map was calculated from the final refined structure with phase contributions from CK-666 omitted.

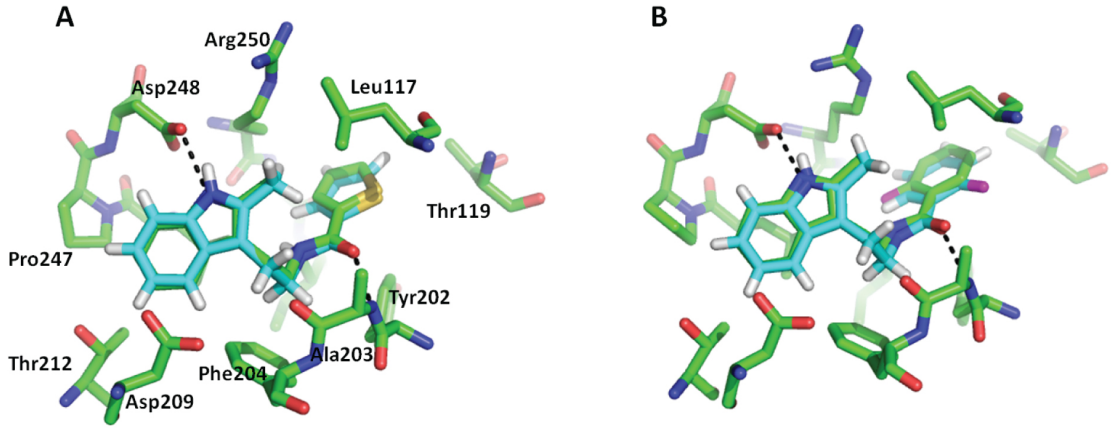

Supplementary Figure 2: Comparison of the docked (cyan) and the observed crystal structure (green) for the complex of Arp2/3 with inhibitor (A) **12** and (B) **1**. The RMSD for heavy atoms is 0.31 Å for **12** and 0.42 Å for **1**. The fluorine atom is displayed in magenta. Residues Gly187 and Ser188 have been omitted for clarity.

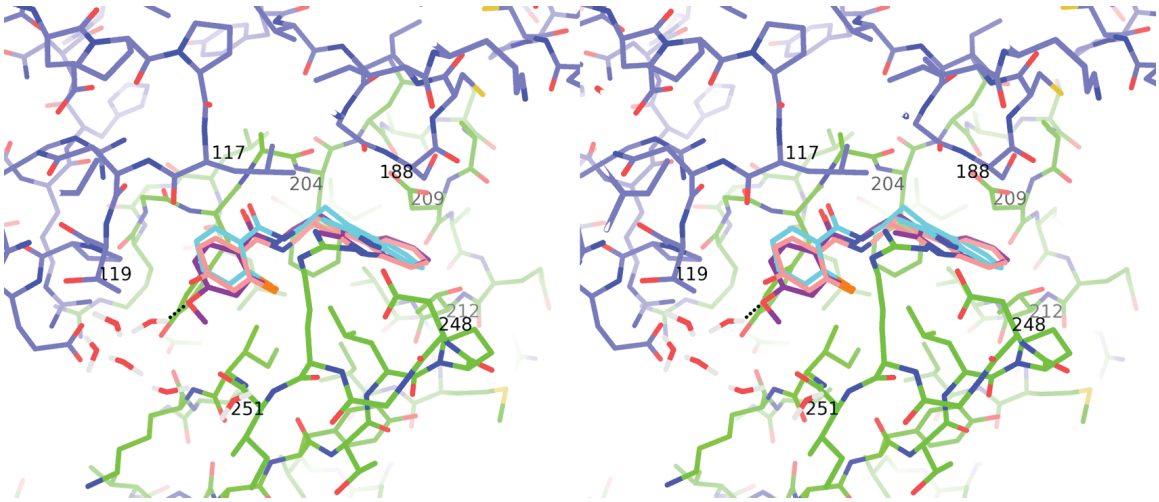

Supplementary Figure 3: Binding pocket with bound **1**, **2** and **4** showing the effect of hydroxyl and methoxy substituents at the R_4 position. Compound **1** (cyan) and the FEP poses of **2** (pink) and **4** (purple) shown in the binding pocket of Arp3 (blue) and Arp2 (green) from the crystal structure of Arp2/3 with bound **1** (3UKR.pdb, light blue).

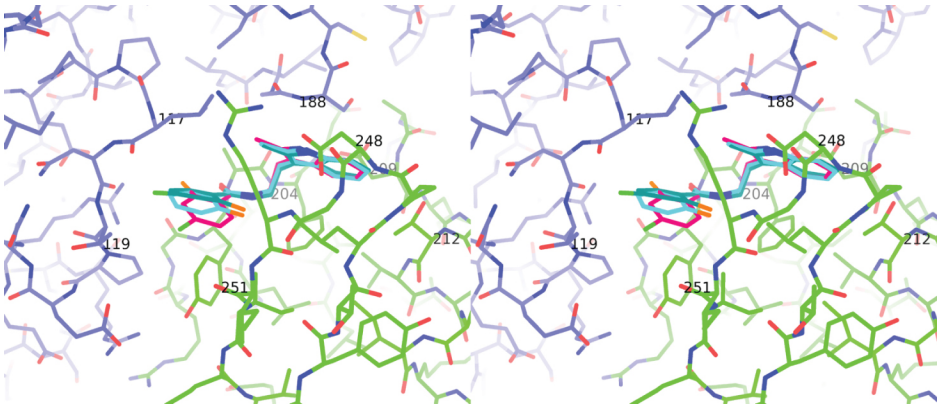

Supplementary Figure 4: Binding pocket with bound **1** and **6** showing the effect of a chlorine substituent at the R_4 position. Compound **1** (cyan) and the FEP pose (dark blue) and Glide docked pose of **6** (magenta) are shown bound to Arp3 (blue) and Arp2 (green) from the crystal structure of Arp2/3 with bound **1** (3UKR.pdb).

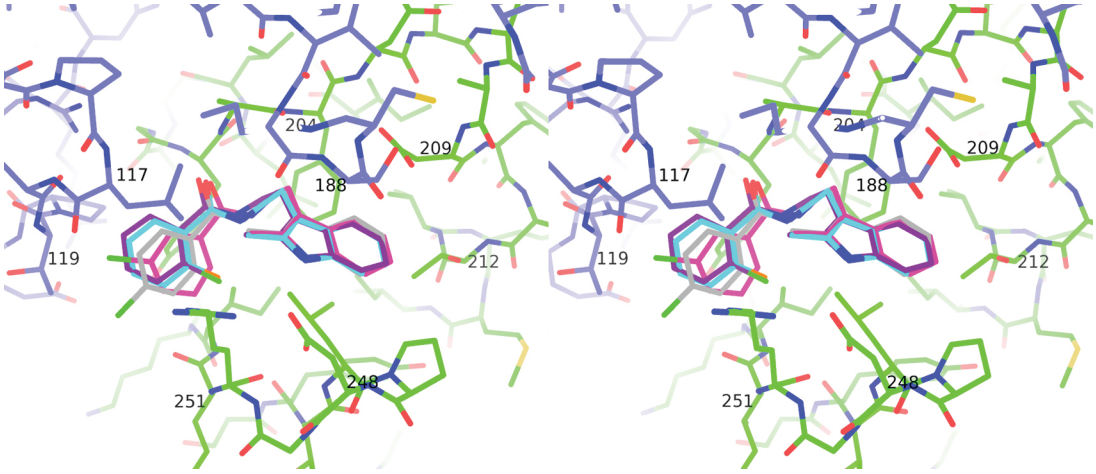

Supplementary Figure 5: Binding pocket with bound **1, 7, 10** and **11** showing the effect of a mono-chloro substitutions on the benzene ring. Compound **1** (cyan) and the FEP poses of **7** (grey), **10** (purple) and **11** (magenta) are shown bound to Arp3 (blue) and Arp2 (green) from the crystal structure of Arp2/3 with bound **1** (3UKR.pdb).

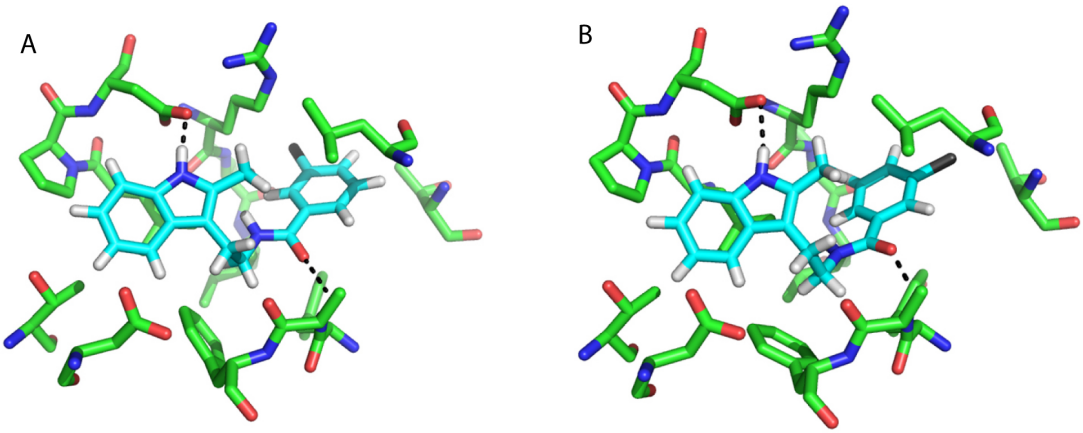

Supplementary Figure 6: The two equivalent positions of the chlorine substitution for compound 11. In (A), the chloro substituent (colored in dark green) points toward Arg250 and is mutated to hydrogen with a ΔΔG=2.52 kcal/mol, while in (B) the chloro substituent points to Thr119 and is mutated to hydrogen with a ΔΔG=2.58 kcal/mol.